Effect of Kerr nonlinearity on an Airy beam

Rui-Pin Chen,[1,*] Chao-Fu Yin,[2] Xiu-Xiang Chu,[1] and Hui Wang[2]

[1]*School of Sciences, Zhejiang A & F University, Lin'an, Zhejiang 311300, China*
[2]*Institute of information optics, Zhejiang Normal University, Jinhua, Zhejiang 321004, China*

The effect of Kerr nonlinearity on an Airy beam is investigated by using the nonlinear Schrödinger equation. Based on the moments method, the evolution of the Airy beam width in the rms sense is analytically described. Numerical simulations indicate that the central parts of the major lobe of the Airy beam initially give rise to radial compression during propagation in a focusing medium, even though the rms beam width broadens. The partial collapse of the center parts of the major lobe of the beam appear below the threshold for a global collapse. The evolutions of the field distributions of the Airy beams are different during propagation in different Kerr media while the beams still travel along the parabolic trajectory just as the beam propagates in free space.

I. INTRODUCTION

The original Airy wave packets introduced by Berry and Balazs in the context of quantum mechanics contain infinite energy [1]. Recently, Siviloglou and Christodoulides [2,3] extended the model by introducing a finite-energy Airy beam for the generation of optical Airy beams. Since then, the Airy beam has been studied extensively [4–10]. These investigations confirmed the unique features of the beam such as diffraction-free and transverse acceleration [2–4], self-healing [5], sorting microscopic particles [6], linear and angular momentum, the Poynting vector [7], nonlinear generation and manipulation [8] of the Airy beam, and changing the phase-matching condition to switch the acceleration direction and the wavelength of the output Airy beam [9] have been studied. Polynkin *et al.* studied the filamentation of femtosecond laser Airy beams in air [10] and in water [11]. Kasparian and Wolf elaborated the transverse energy fluxes of the Airy beam where Kerr nonlinearity plays an important role [12] and the traces of Airy beams carrying high intensities [13]. They found that the traces of the plasma channels roughly follow that of the Airy beam and the Kerr lens induces transverse energy fluxes much larger than the Airy "prism" at the main peak [10–13]. The nonlinear Airy states in photorefractive media with diffusion nonlinearity were studied by Jia *et al.* [14]. These works show the interesting properties and potential applications of Airy beams in the nonlinear optics regime [8–14]. In this work, we study the propagation of the Airy beams in a Kerr medium using the nonlinear Schrödinger (NLS) equation. Because of the complexity of evolution of Airy beams in a Kerr medium, we apply the moments method [15–19], which provides a convenient and rigorous way of obtaining the evolution of the relevant parameters, without any assumption of the solution, to obtain important information about the Kerr effect on the Airy beam. An analytical description of the evolution of the beam width of an Airy beam in the rms sense is obtained. The critical powers of the Airy beams as a function of the beam parameters a_x and a_y that are associated with the modulating part of the Airy beams are analytically obtained. By using numerical simulations for the nonlinear dynamics of the beams in the Kerr

medium, it is found that the central parts of the major lobe of the Airy beam initially give rise to radial compression during propagation in focusing media even though the rms beam width remains constant or broadens. With increasing initial power, the central parts of the major lobe of the Airy beam appear partially collapsed [19–21] while the rms beam width still increases or remains constant. The field distributions of the Airy beam are different during propagation in different Kerr media but the beam still travels along the parabolic trajectory just as when the beam propagates in free space. The intensity distribution of the central parts of the Airy beam increases when the beam propagates in a focusing medium, and the intensity distribution of the sides of the Airy beam decreases in comparison with that of the beam during propagation in free space. When the beam propagates in a defocusing medium, the intensity distribution of the central parts of the Airy beam decreases and the intensity distribution of the sides of the Airy beam increases in comparison with that of the beam during propagation in free space. These results are consistent with the results of the works of Polynkin and Kasparian [10–13].

II. THE MOMENTS METHOD ANALYSIS

The propagation of a light beam in a Kerr medium is described in the paraxial approximation by a NLS equation:

$$\frac{\partial^2 E}{\partial x^2} + \frac{\partial^2 E}{\partial y^2} - 2ik\frac{\partial E}{\partial z} + \frac{2n_2 k^2}{n_0}|E|^2 E = 0, \qquad (1)$$

where k is the linear wave number, n_0 is the linear refraction index of the medium, n_2 is the third-order nonlinear coefficient, x and y are the transverse coordinates, and z is the longitudinal coordinate, respectively. Since a general solution of this problem cannot be given, in this section we apply the moments method to obtain the nonlinear dynamics information about the Kerr effect on the Airy beam by analyzing the evolution of several integral quantities derived from the NLS equation. A definition of these quantities is

$$I_1(z) = \iint_s |E|^2 \, dx dy, \qquad (2a)$$

$$I_2(z) = \iint_s (x^2 + y^2)|E|^2 \, dx dy, \qquad (2b)$$

*chenrp123@163.com

$$I_3(z) = \frac{i}{k} \iint_s \left[x \left(E \frac{\partial E^*}{\partial x} - E^* \frac{\partial E}{\partial x} \right) \right.$$
$$\left. + y \left(E \frac{\partial E^*}{\partial y} - E^* \frac{\partial E}{\partial y} \right) \right] dx dy, \qquad (2c)$$

$$I_4(z) = \frac{1}{2k^2} \iint_s \left(\left| \frac{\partial E}{\partial x} \right|^2 + \left| \frac{\partial E}{\partial y} \right|^2 - \frac{k^2 n_2}{n_0} |E|^4 \right) dx dy. \qquad (2d)$$

The quantities are associated with the beam power (I_1), the beam width (I_2), the momentum (I_3), and the Hamiltonian (I_4) and they satisfy a closed set of coupled ordinary differential equations; thus [15,16], $dI_1(z)/dz = 0$, $dI_2(z)/dz = I_3(z)$, $dI_3(z)/dz = 4I_4(z)$, and $dI_4(z)/dz = 0$. With the important invariant under evolution, $Q = 2I_4 I_2 - I_3^2/4$, one obtains an Ermakov-Pinney [22] equation describing the dynamics of the scaled beam width:

$$\frac{d^2 I_2^{1/2}(z)}{dz^2} = \frac{Q}{I_2^{3/2}(z)}. \qquad (3)$$

For a finite-power Airy beam as an initial field distribution [1–3],

$$E(x, y; z = 0)$$
$$= A_0 \text{Ai}(x/x_0) \exp(a_x x/x_0) \text{Ai}(y/x_0) \exp(a_y y/x_0), \qquad (4)$$

where A_0 is the amplitude of the complex amplitude $E(x, y, z = 0)$, x_0 is an arbitrary transverse scale, and a_x and a_y are small positive parameters. The general solution of Eq. (3) with the Airy beam as an initial field distribution can be given [22] as

$$I_2(z) = I_2(z = 0) + \frac{Q}{I_2(z = 0)} z^2, \qquad (5)$$

where

$$Q = \frac{(3 + 8a_y^3 + 16a_y^6)a_x^2 + (3 + 8a_x^3 + 16a_x^6)a_y^2}{128\pi \sqrt{a_x a_y} a_x^2 a_y^2} 2A_0^4 x_0^4$$
$$\times \left[\frac{a_x + a_y}{32k^2(a_x a_y)^{3/2}} \exp\left(\frac{4a_x^3 + 4a_y^3}{3} \right) - \frac{n_2 A_0^2 x_0^2}{2n_0} \right.$$
$$\left. \times \frac{K_0(2a_x^3) K_0(2a_y^3)}{32\pi^3} \exp\left(\frac{12a_x^3 + 12a_y^3}{3} \right) \right]. \qquad (6)$$

It should be noted that the Fourier transform and Parseval's formula have been used for calculating these quantities. Equation (5) describes the variation of the scaled beam width of the Airy beam in a Kerr medium. For a better expression of the dependence on the nonlinearity, P_{cr} is defined as the critical power required to collapse the beam with a uniform wave front [18]. When $Q = 0$, the rms beam width remains constant, as recognized from Eq. (5). Then the critical value of I_1 can be obtained from Eq. (6) and the critical power can be obtained by $P_{cr} = n_0 c \varepsilon_0 I_1/2$ for the Airy beam to yield

$$P_{cr} = \frac{c \varepsilon_0 \pi^2 n_0^2}{8k^2 n_2} \frac{a_x + a_y}{a_x^2 a_y^2 K_0(2a_x^3) K_0(2a_y^3) \exp(2a_x^3 + 2a_y^3)}, \qquad (7)$$

where c is velocity of light in vacuum and ε_0 is the permittivity of free space. The value of the critical power of the Airy
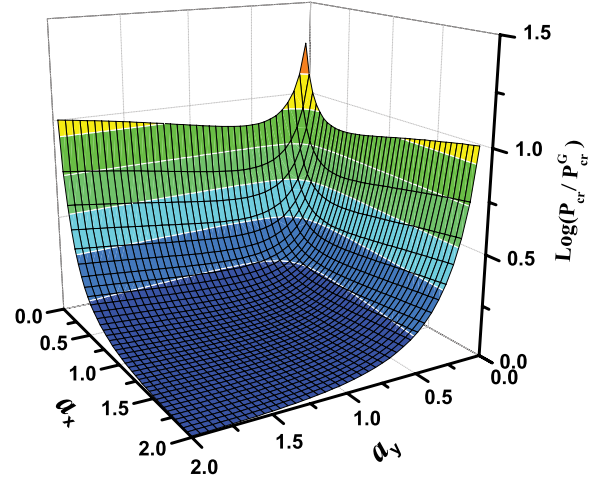

FIG. 1. (Color online) The critical powers of the Airy beam for different a_x and a_y.

beam is only dependent on the beam profile of the transverse distribution and the nonlinear parameters of the medium. $K_0(x)$ is the modified Bessel function of the second kind and can be expanded as follows:

$$K_0(x) = \sqrt{\frac{\pi}{2x}} \exp(-x) \left[\sum_{k=0}^{n-1} (-1)^n \frac{\Gamma(k + 1/2)}{k! \Gamma(-k + 1/2)} (2x)^{-k} \right.$$
$$\left. + O(|x|^{-n}) \right], \qquad (8)$$

where $\Gamma(\cdot)$ is the gamma function. When a_x and a_y tend to infinity, in this case, n take the value of 1. Substituting Eq. (8) into Eq. (7), the critical power of the Airy beam reduces to the critical power of the Gaussian beam:

$$P_{cr}^G = \frac{\pi c \varepsilon_0 n_0^2}{n_2 k^2}, \qquad (9)$$

where the critical power of a Gaussian beam, P_{cr}^G, can also be obtained by performing the preceding process with a Gaussian profile as an initial field distribution. Figure 1 shows the logarithmic scale of the ratio of the critical powers of the Airy beams to that of the Gaussian beam. As recognized from Fig. 1, the critical powers of the Airy beams increase with decreasing modulating parameters a_x and a_y, and the values of the critical powers of the Airy beams tend the critical power of a Gaussian when a_x and a_y tend to infinity. Obviously, the resulting powers, P_{cr}, is thus the upper bound for the critical power [21]. When the initial power exceeds the critical power P_{cr}, the beam rms width goes to zero in a finite propagation distance as predicted by the moments method, and a global collapse occurs.

III. NUMERICAL SIMULATION AND ANALYSIS

Numerical simulations are carried out by using the Crank-Nicholson finite-difference method [23] to investigate further the Kerr effect on an Airy beam. In the following numerical calculation, we take the wavelength $\lambda = 0.53$ μm, $x_0 = 100$ μm, and $z_0 = kx_0^2/2 = 6$ mm, respectively. The peak intensities as a function of the propagation distance with
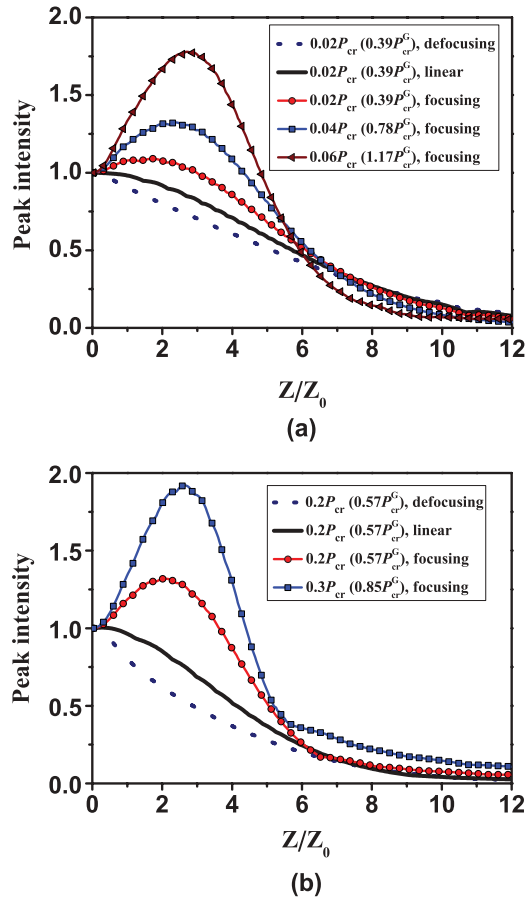
(a)

(b)

FIG. 2. (Color online) The peak intensity of the Airy beam as a function of the propagation distance with different initial powers: (a) $a_x = a_y = 0.1$ and (b) $a_x = a_y = 0.3$.

different initial powers are shown in Fig. 2 for $a_x = a_y = 0.1$ and $a_x = a_y = 0.3$. For the sake of intuition, the initial powers are specified below not only in terms of P_{cr} but also in terms of P_{cr}^G.

The traces have been normalized with respect to their initial peak intensities in Fig. 2. Although the moments method predicts that the rms beam width broadens when the initial power is below the critical power, the peak intensities initially increase, which would suggest that the major lobe of the Airy beams initially compresses. Obviously the rms beam broadens because the departure of each lobe from the beam center more than compensates for the compression of each lobe. The simulations show that, with further increasing initial power, the intensity at the central parts of the major lobe dominate and eventually lead to a collapse [19–21], while the rms beam width still increases or remains constant. By using numerical simulations, we find that the ratio of the initial powers which give rise to partial collapse to the critical power are different with different beam parameters such as the cases shown in Fig. 2(a) for $a_x = a_y = 0.1$ and Fig. 2(b) for $a_x = a_y = 0.3$. The ratio of the initial powers which give rise to partial collapse to the critical power increases with the increasing beam parameters a_x and a_y. Numerical simulations indicate that the partial collapse occurs for $a_x = a_y = 0.1$ when $P_{in} = 0.1P_{cr} = 2.0P_{cr}^G$ and the partial collapse occurs for $a_x = a_y = 0.3$ when $P_{in} = 0.5P_{cr} = 1.4P_{cr}^G$.
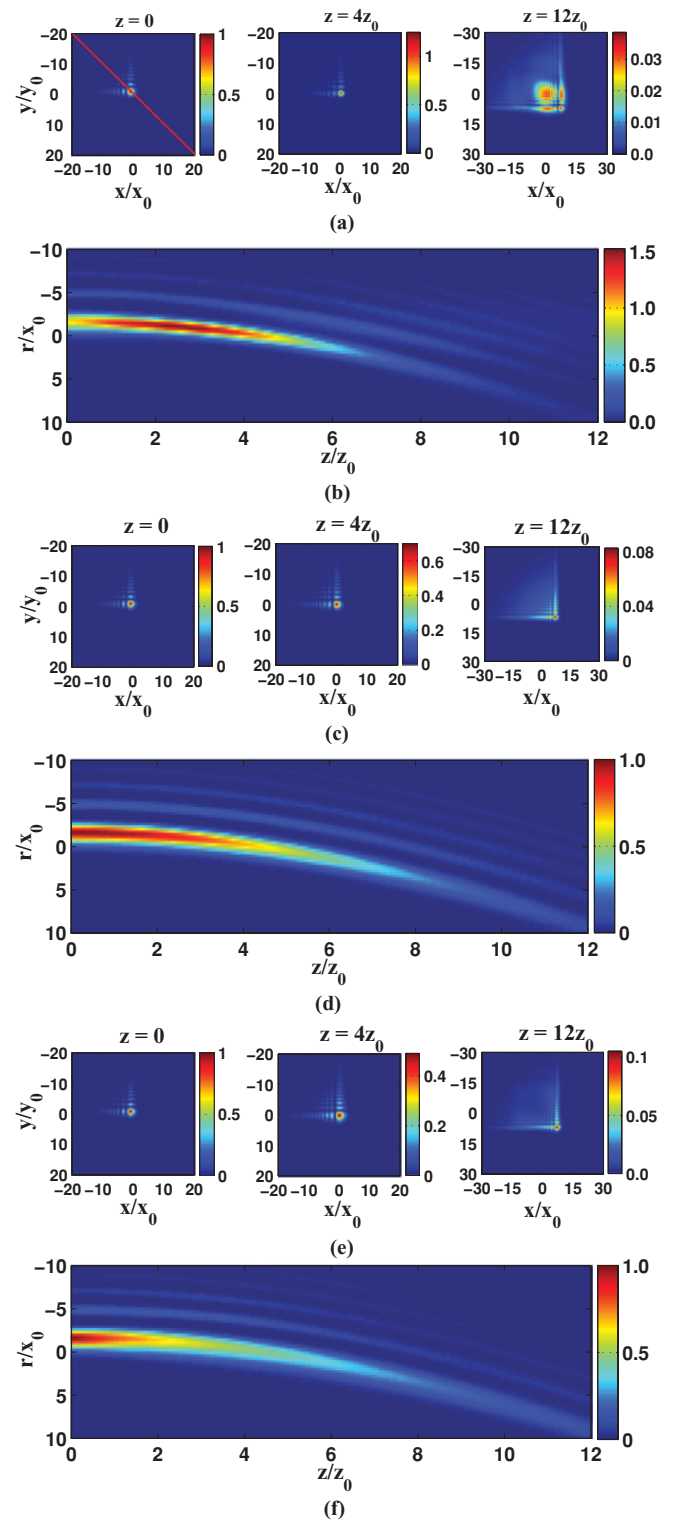

FIG. 3. (Color online) The intensity distribution of an Airy beam ($a_x = a_y = 0.1$) at different propagation distances with initial powers $P_{in} = 0.05P_{cr} = 1.0P_{cr}^G$ in (a, b) focusing medium, (c, d) free space, and (e, f) defocusing medium. The thin (red) line in the first plot indicates the position of the longitudinal cross section.

In order to further illustrate how the beam is evolved, the intensity distributions of the Airy beam in the focusing nonlinear medium with the beam parameters $a_x = a_y = 0.1$ and

initial powers $P_{in} = 0.05P_{cr} = 1.0P_{cr}^G$ at different propagation distances are shown in Figs. 3(a) and 3(b). For comparison, the intensity distributions of the Airy beam with the same beam parameters in free space are shown in Figs. 3(c) and 3(d), and with the defocusing medium in Figs. 3(e) and 3(f). Figures 3(a), 3(c), and 3(e) show the transversal intensity distribution of the Airy beam at propagation distances $z = 4z_0$ and $12z_0$, respectively. Figures 3(b), 3(d), and 3(f) show the evolution of the intensity distribution in the longitudinal cross sections of the Airy beam, which pass through the center of the beam and the major lobe, during propagation in focusing medium, free space, and defocusing medium, respectively. Again, the intensities are normalized with respect to their initial peak intensities. As recognized from Fig. 3, the beams travel along the identical accelerating trajectory during propagation either in the Kerr medium or in free space. The beam profile remains almost constant up to a certain distance during propagation in the Kerr medium just as for propagation in free space [2,3]. The field distributions of the Airy beam are different during propagation in the Kerr medium than in free space. When the beam propagates in a focusing medium, the intensity distribution of the central parts of the Airy beam becomes more intensive and the intensity distribution of the sides of the Airy beam becomes weaker than that of the beam during propagation in free space. Numerical simulations indicate that the intensity distribution of the central parts of the Airy beam exceed the intensity distribution of the sides of the Airy beam, including the major lobe of the beam, after the beam propagates a certain distance, although the beam profile still remains invariant just as when the beam propagates in free space, as shown in Fig. 3(a). When the beam propagates in a defocusing medium, the intensity distribution of the central parts of the Airy beam becomes weaker and the intensity

distribution of the sides of the Airy beam becomes more intensive than that of the beam during propagation in free space, as shown in Fig. 3(e). These results confirm that the rms beam width of the Airy beam in free space is bigger than that in the focusing medium but less than that in the defocusing medium, although the propagation traces and beam profiles are identical. These results are in agreement with the analytical expression of Eq. (5) and are consistent with the results of the works of Polynkin and Kasparian [10–13].

IV. CONCLUSION

The effect of the Kerr nonlinearity on an Airy beam has been studied by using the NLS equation. The evolution of the Airy rms beam width has been analytically described. The analytical expression of the critical powers for different parameters a_x and a_y is given. By using numerical simulations, the dynamic interaction between nonlinear focusing and linear diffraction has been analyzed. It has been found that the partial collapse of the major lobe of the Airy beam appears when the initial power is still below the critical collapse power. The beam profile remains almost constant during propagation, either in the Kerr medium or in free space for a certain distance. The field distribution of the Airy beam differs during propagation in different nonlinear media.

[1] M. V. Berry and N. L. Balazs, Am. J. Phys. **47**, 264 (1979).

[2] G. A. Siviloglou, J. Broky, A. Dogariu, and D. N. Christodoulides, Phys. Rev. Lett. **99**, 213901 (2007).

[3] G. A. Siviloglou and D. N. Christodoulides, Opt. Lett. **32**, 979 (2007).

[4] M. A. Bandres and J. C. Gutierrez-Vega, Opt. Express **15**, 16719 (2007).

[5] J. Broky, G. A. Siviloglou, A. Dogariu, and D. N. Christodoulides, Opt. Express **16**, 12880 (2008).

[6] J. Baumgartl, M. Mazilu, and K. Dholakia, Nat. Photonics **2**, 675 (2008).

[7] H. I. Sztul and R. R. Alfano, Opt. Express **16**, 9411 (2008).

[8] T. Ellenbogen, N. Voloch-Bloch, A. Ganany-Padowicz, and A. Arie, Nat. Photonics **3**, 395 (2009).

[9] I. Dolev, T. Ellenbogen, and A. Arie, Opt. Lett. **35**, 1581 (2010).

[10] P. Polynkin, M. Kolesik, J. Moloney, G. A. Siviloglou, and D. N. Christodoulides, Science **324**, 229 (2009).

[11] P. Polynkin, M. Kolesik, and J. Moloney, Phys. Rev. Lett. **103**, 123902 (2009).

[12] J. Kasparian and J. P. Wolf, J. Eur. Opt. Soc. **4**, 09039 (2009).

[13] J. Kasparian and J. P. Wolf, Science **324**, 194 (2009).

[14] S. Jia, J. Lee, J. W. Fleischer, G. A. Siviloglou, and D. N. Christodoulides, Phys. Rev. Lett. **104**, 253904 (2010).

[15] V. M. Prez-Garcia, P. Torres, and G. D. Montesinos, SIAM J. Appl. Math. **67**, 990 (2007).

[16] J. J. Garcia-Ripoll, V. M. Perez-Garcia, and P. Torres, Phys. Rev. Lett. **83**, 1715 (1999).

[17] M. Centurion, M. A. Porter, P. G. Kevrekidis, and D. Psaltis, Phys. Rev. Lett. **97**, 033903 (2006).

[18] C. Pare and P. A. Blanger, Opt. Quantum Electron. **24**, S1051 (1992).

[19] P. Johannisson, D. Anderson, M. Lisak, and M. Marklund, Opt. Commun. **222**, 107 (2003).

[20] G. Fibich and B. Ilan, J. Opt. Soc. Am. B **17**, 1749 (2000).

[21] G. Fibich and A. L. Gaeta, Opt. Lett. **25**, 335 (2000).

[22] V. P. Ermakov, Appl. Anal. Discrete Math. **2**, 123 (2008).

[23] W. H. Press, S. A. Teukolsky, W. T. Vetterling, and B. P. Flannery, *Numerical Recipes: The Art of Scientific Computing*, 3rd ed. (Cambridge University Press, New York, 2007), Chap. 20, p. 1024.